

Role of the Electron Temperature in the Current Decay during Disruption in JT-60U^{*)}

Yoshihide SHIBATA, Akihiko ISAYAMA, Go MATSUNAGA, Yasunori KAWANO, Seiji MIYAMOTO¹⁾, Victor LUKASH²⁾, Rustam KHAYRUTDINOV³⁾ and JT-60 team

Japan Atomic Energy Agency, Naka 319-0193, Japan

¹⁾*Research Organization for Information Science and Technology, Tokai-mura 319-1106, Japan*

²⁾*Kurchatov Institute, Moscow, Russia*

³⁾*Troitsk Institute for Innovation and Fusion Research, Moscow, Russia*

(Received 9 December 2013 / Accepted 11 April 2014)

The effect of the electron temperature T_e on the plasma current decay after the mini-collapse was investigated for the disruption in JT-60U owing to a massive neon gas puff by using the disruption simulation code DINA. During the current quench in JT-60U, the fast electron temperature decrease is followed by a transient plasma current increase. This is called “mini-collapse”, typically occurring when the plasma current decreases to 80–90% of its value at the flattop phase. The plasma evolution after the mini-collapse was investigated using the DINA code for three assumed T_e profiles: flat, broad, and peaked profiles. The time evolution of the plasma current, plasma center position, plasma cross section, and vacuum vessel current were not found to be sensitive to the T_e profile after the mini-collapse. The plasma current after mini-collapse decreased owing to the plasma resistance, although it was previously found that the plasma current decrease during the initial phase of current quench was owing to the time derivative of the plasma inductance [Y. Shibara *et al.*, Nucl. Fusion **50**, 025065 (2010)].

© 2014 The Japan Society of Plasma Science and Nuclear Fusion Research

Keywords: disruption, current quench, DINA code, electron temperature, plasma resistance

DOI: 10.1585/pfr.9.3402084

1. Introduction

Disruption is extremely critical in ITER and DEMO reactor. Methods to mitigate and prevent disruption have been developed for many tokamak devices [1]. However, no such techniques have been established yet for ITER and DEMO reactor.

Large eddy and halo currents induced by current quench (CQ) owing to the disruption may seriously damage the vacuum vessel and in-vessel components [1]. In ITER and DEMO reactor, the simulations of disruption are used to predict the damage caused by disruption in the design of the fusion devices. Many disruption simulation codes have been developed; e.g., DINA [2] and TSC [3] are for asymmetric simulations, while M3D [4] and NIMROD [5] are for non-asymmetric simulations.

The validation of DINA code with experimental data for disruption has been carried out for JET [6], JT-60U [7], and MAST [8]. In the JT-60U validation [7], the plasma current I_p calculated with the DINA code well agreed with the experimental data measured with a Rogowskii coil. However, other plasma parameters (e.g., major and minor radii, plasma cross-section, and so on) were not compared in these validations. In the DINA code, the electron

temperature T_e profile during the CQ was assumed spatially constant and calculated from the energy balance [2]. However, it was observed that the T_e profile in the core region was greater than 400 eV immediately after the thermal quench in JT-60U [9]. In this case, time derivative of the plasma inductance dL_p/dt was reported to be important for determining the current decay time during the initial phase of the CQ from 100–90% of I_p immediately before disruption. The validation of the DINA code using experimental data was carried out during the initial phase of the CQ in JT-60U caused by massive neon gas puff [10]. In addition, the time change of the T_e profile was important for establishing the plasma current decay.

During the CQ in JT-60U, a fast decrease in the electron temperature followed by a transient increase in the plasma current was observed. This is called “mini-collapse”, typically occurring when the I_p decreases to 80–90% of the value at the flattop phase in JT-60U. In addition, the T_e after the mini-collapse was not measured because the T_e was below the limit of electron cyclotron emission (ECE) measurement. To clarify the mechanism for the current decay time for entire CQ period, we need to investigate the effect of T_e on the plasma current decay after the mini-collapse. In this study, we calculated the time evolution of I_p , the plasma center position, L_p , and the vacuum vessel

author's e-mail: shibata.yoshihide@jaea.go.jp

^{*)} This article is based on the presentation at the 23rd International Toki Conference (ITC23).

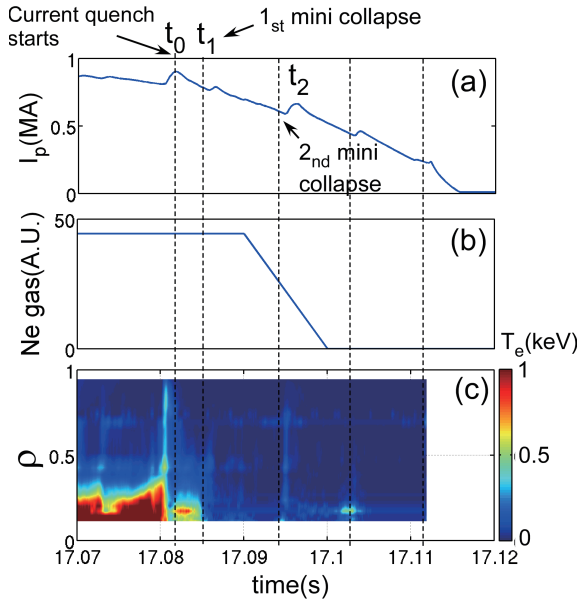


Fig. 1 Time evolution of the (a) plasma current I_p , (b) an amount of massive neon gas puff, and (c) the electron temperature T_e profile measured by ECE measurement.

current using the DINA code and assuming several T_e profiles. Finally, we compared the results of the calculations with the experimental data.

2. Experiment

Figure 1 shows the time evolution of I_p , the amount of massive neon gas puff, and the T_e profile obtained with the ECE measurement. In the discharge, the toroidal magnetic field is 2.268 T, the safety factor of the plasma surface is 6.05, and the poloidal beta is 0.2 immediately before disruption. The line averaged electron density n_e gradually increased and the stored energy decreased after the massive neon gas puff [9]. The CQ started at $t = t_0$ with many mini-collapses occurring during the CQ. In the initial phase of CQ ($t_0 \sim t_1$), T_e had a profile and the value in the plasma center was ~ 600 eV. Subsequently, in the first mini-collapse at $t = t_1$, T_e rapidly fell below the ECE measurement limit of 100 eV.

Figure 2 shows the time evolution of L_p , the plasma major radius R_0 , the vertical position Z_0 , and the plasma cross-section S calculated with the Cauchy Condition Surface (CCS) code including the vacuum vessel (VV) current [11, 12]. L_p consists of the plasma internal inductance L_i and the plasma external inductance L_e . L_p is evaluated with the following equation:

$$\begin{aligned} L_p &= L_i + L_e \\ &= \mu_0 R_0 l_i / 2 + \mu_0 R_0 (\ln(8R_0/a) - 2), \end{aligned} \quad (1)$$

where μ_0 is a magnetic permeability, l_i is the internal inductance, and a is a minor radius. In the CCS code, l_i is calculated with the following equation,

$$l_i = 2(\Lambda - \beta_p), \quad (2)$$

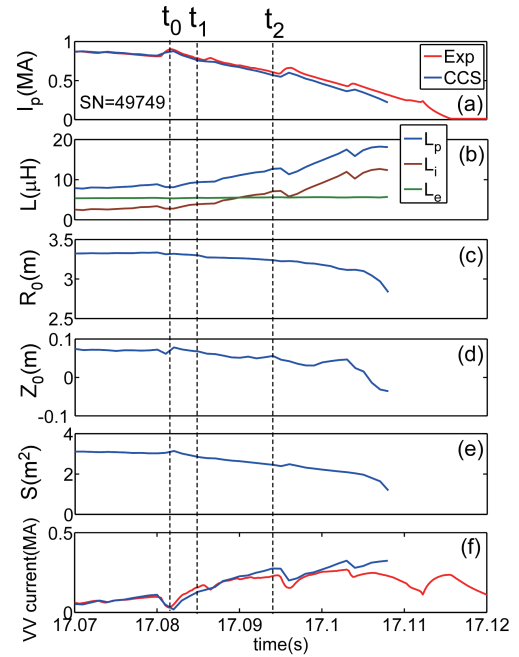


Fig. 2 Time evolution of the (a) plasma current I_p , (b) plasma inductance L_p , plasma internal L_i and external inductance L_e , (c) the plasma major radius R_0 , (d) vertical position Z_0 , (e) plasma cross-section S , and (f) vacuum vessel current. Red lines are measured by using the Rogowskii coil and the blue lines are calculated by using the CCS code.

where Λ and β_p are the Shafranov lambda and poloidal beta, respectively. The Shafranov lambda is evaluated by integrating the magnetic field components on the plasma boundary in the CCS code. The poloidal beta is obtained by measuring the magnetic sensor. In this study, the time change of β_p is neglected because the time change and absolute value of β_p are quite small during the CQ. The plasma and VV currents were measured with a Rogowskii coil. The plasma and VV current calculated using the CCS code well agreed with the measured values. After the first mini-collapse at $t = t_1$, R_0 , Z_0 , and S gradually decreased. L_p , especially the L_i , was increased after the first mini-collapse.

3. Simulation and Discussion

The disruption simulation code DINA is a two-dimensional free-boundary equilibrium evolution code that includes the poloidal field (PF) coils and surrounding conducting structure. In the simulation, the PF coil current in experiment was input in the DINA code. The n_e is calculated by using the energy balance, assuming it is spatially constant. The effective charge profile is $Z_{\text{eff}} = 4(1 - \rho^2) + 1$, which is based on the calculation results using the neon fraction in ref [9].

The comparison between the calculated and experimental plasma parameters was performed. The compared plasma parameters are as follows: Direct measurement is I_p , VV current, and loop voltage V_{loop} using flux loop lo-

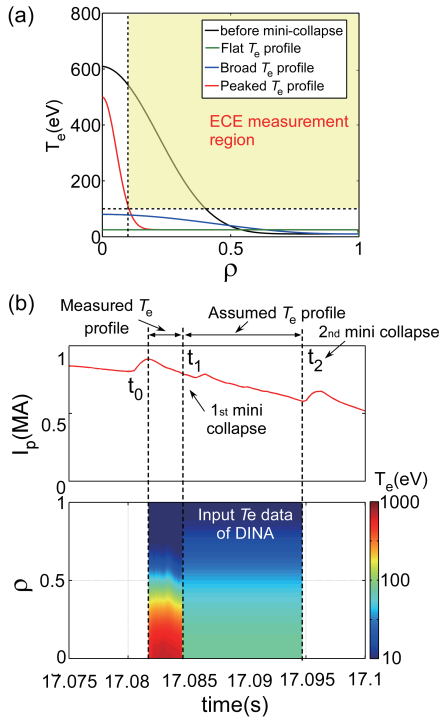


Fig. 3 (a) Assumptions of several T_e profile in DINA simulation. (b) The time evolutions of plasma current and the input data of T_e profile in DINA simulation.

cated in high field side (HFS) of toroidal magnetic field at $Z_0 = 0.14$ m: CCS code is R_0 , Z_0 , and S .

Three T_e profile types were assumed to investigate the effect of T_e on the current decay time after the first mini-collapse. Figure 3 (a) shows the assumed T_e profiles. After the first mini-collapse ($t_1 \sim t_2$), T_e was assumed by the following equation:

$$T_e(\rho) = (T_{e0} - T_{e\text{-edge}})(1 - \rho^2)^\kappa + T_{e\text{-edge}}, \quad (\text{in eV}) \quad (3)$$

where T_{e0} is the T_e in the plasma center, κ is the peak index of the T_e profile, and $T_{e\text{-edge}}$ is the T_e in the edge region. The DINA code calculations started at $t = t_0$. The measured T_e profile using the ECE was used until the first mini-collapse ($t_0 \sim t_1$). After the first mini-collapse ($t_1 \sim t_2$), the assumed T_e profile by using Eq. (3) is shown in Fig. 3 (b). In the simulation, the time change of the assumed T_e profile was not considered.

The time evolution of the plasma current was reproduced by using the following assumed T_e profiles: the flat T_e profile parameters are $T_{e0} = 25$ eV and $\kappa = 0$; the broad T_e profile parameters are $T_{e0} = 80$ eV, $\kappa = 3$, and $T_{e\text{-edge}} = 10$ eV; the peaked T_e profile parameters are $T_{e0} = 500$ eV, $\kappa = 170$, and $T_{e\text{-edge}} = 25$ eV. Figure 4 shows the time evolution of I_p , V_{loop} , VV current, R_0 , Z_0 , S , and L_p in each assumed T_e profile. In the flat T_e profile (green line), most of the plasma parameters were reproduced with the DINA code. Only L_p differed for DINA and CCS code calculations. The L_p decreased after the mini-collapse at

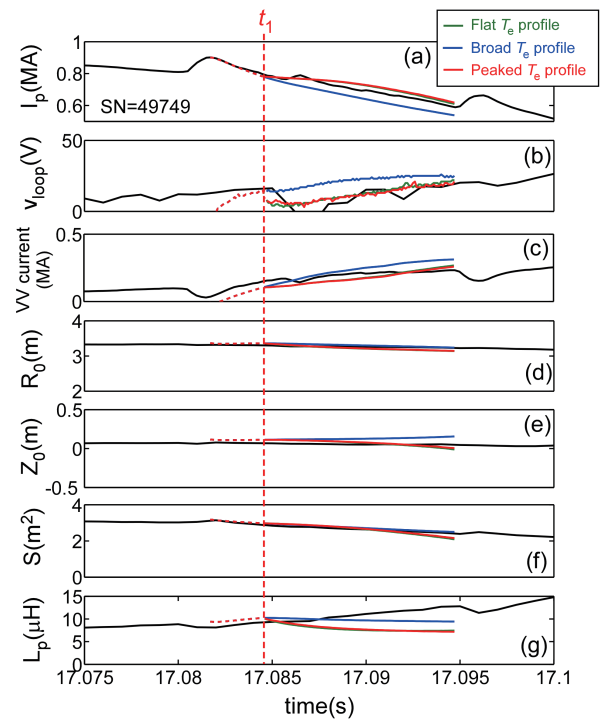


Fig. 4 Time evolutions of (a) plasma current I_p , (b) loop voltage V_{loop} , (c) VV current, (d) major radius R_0 , (e) the vertical position Z_0 , (f) plasma cross section S , and (g) plasma inductance L_p .

$t = t_1$. Figure 5 (a) shows the time evolution of the current density j profile calculated by using the flat T_e profile. The j profile changed from peaked to flat profile in this case. Hence L_p decreased in the flat T_e profile.

In the broad T_e profile (blue line), the plasma parameters in Fig. 5 reproduce the experimental values that are common with flat T_e profile in Fig. 4. The results suggest that the behavior of plasma parameters (I_p , VV current, R_0 , Z_0 , and S) is not sensitive to the T_e profile when the T_e profile is lower than 100 eV. The j was the peaked profile at the center after the mini-collapse, as shown in Fig. 5 (b). The calculated and experimental L_p and V_{loop} values differed in the simulation. The L_p decreased because the plasma current density in the plasma center gradually decreased.

In the peaked T_e profile (red line), the plasma parameters had values close to those of the flat T_e profile. In this case, j peaked for $\rho < 0.1$ because the T_e in the plasma center was much higher than one in the edge region as shown in Fig. 5 (c). For $\rho > 0.1$, j changed to the flat profile similar to the flat T_e profile case. Therefore, the DINA simulation suggest that T_e in the plasma center does not affect the plasma parameters and L_p . The DINA code did not reproduce the increase in L_p , whereas it reproduced other plasma parameters (I_p , VV current, R_0 , Z_0 , and S).

The increase in the plasma inductance after the mini-collapse at $t = t_1$ was not reproduced using the DINA code and assumed T_e profiles. However, I_p decreased after the mini-collapse in the DINA simulations. Figure 6 shows the

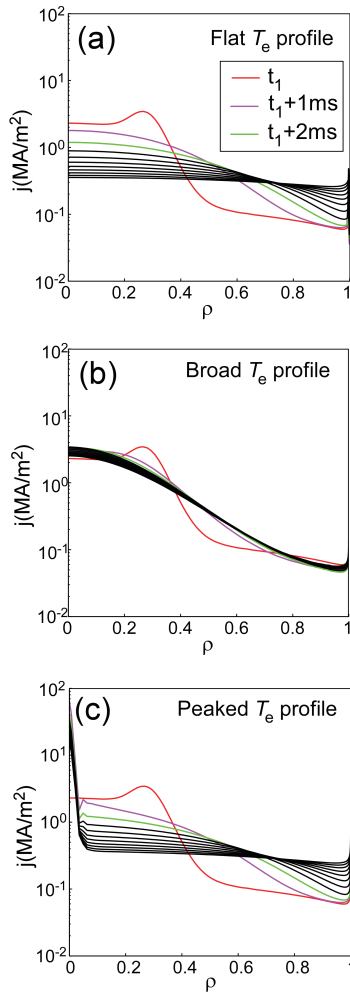


Fig. 5 Time evolution of the current density j profile in the case of (a) flat, (b) broad, and (c) peaked T_e profiles.

time evolution of I_p profile in each assumed T_e profile. I_p profile $\Delta I_p(\rho)$ was evaluated by the following equation:

$$\Delta I_p(\rho) = \int_{\rho_1}^{\rho_2} j(\rho) dS, \quad (4)$$

where $j(\rho)$ is the current density profile, and $\rho_2 - \rho_1 = 0.06$. In the DINA calculations using the broad T_e profile, I_p mainly decreased for $\rho = 0.3$. Therefore, in this case, I_p decreased because of the plasma resistance R_p near $\rho = 0.3$. The time evolution of ΔI_p in the peaked T_e profile was similar to that in the flat T_e profile. For $\rho = 0.3$, I_p was rapidly decreased, whereas I_p in the edge region increased. In these cases, I_p was diffused into the plasma edge region. In the peaked T_e profile, the effect of peak of I_p in the plasma center is small. Therefore, in these DINA simulations, the plasma current decay was determined by the R_p in middle and edge regions.

4. Conclusion

The effect of electron temperature T_e on the plasma current decay after the mini-collapse during the CQ was

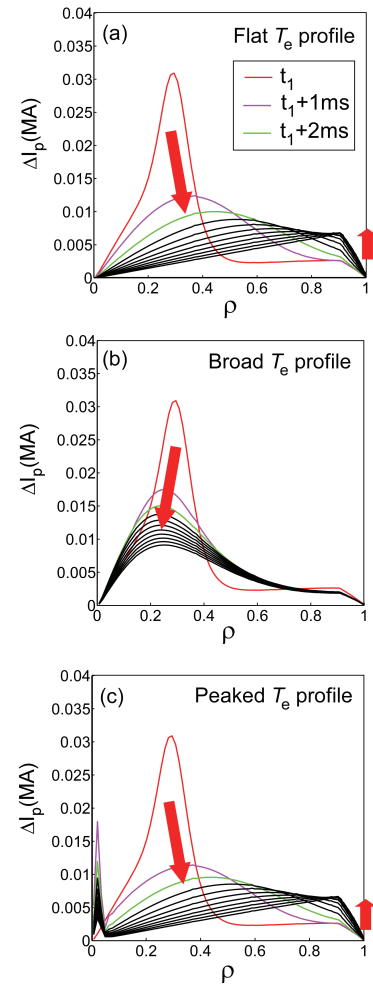


Fig. 6 Time evolution of plasma current profile in the case of (a) flat, (b) broad, and (c) peaked T_e profiles.

investigated using the DINA code and assuming several T_e profiles during disruption in JT-60U owing to massive neon gas puff. The estimated T_e after the mini-collapse was lower than 100 eV because the ECE was below the detection limit of its measurement. The plasma current was reproduced by using the following assumed T_e profiles: flat, broad, and peaked. The DINA simulations suggest that the time evolution of the plasma current, the position of plasma center, the plasma cross-section, and the VV current are not sensitive to the T_e profile when the T_e profile was lower than 100 eV. In these cases, the plasma current after the mini-collapse decreased owing to the plasma resistance in the middle and edge regions, although the plasma current during the initial phase of the CQ decreased owing to the time derivative of the plasma inductance. The increase in the plasma inductance estimated with the CCS code during the CQ was not reproduced with the DINA code because the current density profile becomes flat when the T_e profile was lower than 100 eV. In the future, we need to investigate the reason why the plasma inductance evaluated with the CCS code is not reproduced by the DINA code after the mini-collapse.

- [1] T.C. Hender *et al.*, Nucl. Fusion **47**, S128-202 (2007).
- [2] R. Khayrutdinov *et al.*, J. Computational Phys. **109**, 193 (1993).
- [3] S.C. Jardin *et al.*, J. Comput. Phys. **66**, 481 (1986).
- [4] W. Park *et al.*, Phys. Plasmas **6**, 1796 (1999).
- [5] A. Glasser *et al.*, Plasma Phys. Control. Fusion **41**, A747 (1999).
- [6] V. Lukash *et al.*, Nucl. Fusion **47**, 1476 (2007).
- [7] H. Ohwaki *et al.*, 32nd EPS Conference on Plasma Phys. Tarragona, 27 June-1 July 2005 ECA Vol.29C, P-5.099 (2005).
- [8] Windridge *et al.*, 34th EPS Conference on Plasma Phys. Warsaw, 2-6 July 2007 ECA Vol.31F, P-1.108 (2007).
- [9] Y. Shibata *et al.*, Nucl. Fusion **50**, 025065 (2010).
- [10] Y. Shibata *et al.*, Plasma Phys. Control. Fusion **56**, 045008 (2014).
- [11] K. Kurihara *et al.*, Fusion Eng. Des. **51-52**, 1049 (2000).
- [12] K. Kurihara *et al.*, Fusion Eng. Des. **19**, 235 (1992).